

## Purine Nucleoside Phosphorylase-Catalyzed, Phosphate-Independent Hydrolysis of 2-Amino-6-mercapto-7-methylpurine Ribonucleoside

Jianming Cheng, Victor Farutin,<sup>1</sup> Zhijun Wu,<sup>2</sup> Gayatry Jacob-Mosier,<sup>3</sup>  
Brad Riley, Ryan Hakimi, and Eugene H. Cordes<sup>4</sup>

*College of Pharmacy and Department of Chemistry, University of Michigan,  
Ann Arbor, Michigan 48109*

*Received September 18, 1998*

In the presence of 1 mM phosphate, 2-amino-6-mercapto-7-methylpurine ribonucleoside (MESG) is a well-behaved substrate for calf spleen purine nucleoside phosphorylase (PNP). In the absence of phosphate, calf spleen PNP catalyzes a slow hydrolysis of MESG, which is accompanied by inactivation of the enzyme, analogous to the previously observed PNP-catalyzed hydrolysis of inosine and guanosine with formation, in the former case, of a stable PNP-hypoxanthine complex (P. C. Kline and V. L. Schramm (1992) *Biochemistry* **31**, 5964–5973). Qualitative and semiquantitative features of calf spleen PNP-catalyzed hydrolysis of MESG are accounted for by the following model. First, in the absence of phosphate and at pH 7.4, the enzyme exists as an equilibrium mixture of monomer and trimer with a dissociation constant for the trimer of  $3 \times 10^{14} \text{ M}^2$ . Second, a stoichiometric reaction between three molecules of MESG and the PNP trimer results in the formation of a stable PNP-purinethiol complex. Third, the PNP-purinethiol complex initially formed with the monomeric enzyme partitions between product release and formation of a stable complex with 55 turnovers per inactivation event. Fourth, the stable PNP-purinethiol complexes are rapidly dissociated by phosphate to regenerate active enzyme. This dissociation is accompanied by an increase in absorbance at 356 nm consistent with a  $pK_a$  for the purinethiol base on the enzyme of 8.1, compared to a corresponding value of 8.8 in aqueous solution. © 1999 Academic Press

### INTRODUCTION

Potent and specific inhibitors of purine-nucleoside phosphorylase (purine-nucleoside:orthophosphate ribosyltransferase, EC 2.4.2.1; PNP) have multiple plausible utilities in clinical medicine (2–4). These derive from the demonstration that inherited deficiency of this enzyme is associated with profound immunodeficiency in T-cell function (5,6). It follows that a clinical use might be found for such inhibitors for T-cell lymphomas and leukemias, autoimmune diseases, psoriasis, and prevention of organ graft rejection, among other possibilities.

<sup>1</sup> Present address: Millennium Pharmaceuticals, Inc., 238 Main Street, Cambridge, MA 02142.

<sup>2</sup> Present address: Helios Pharmaceuticals, Inc., Louisville, KY.

<sup>3</sup> Present address: 617 Elmwood Road, Bay Village, OH 44140.

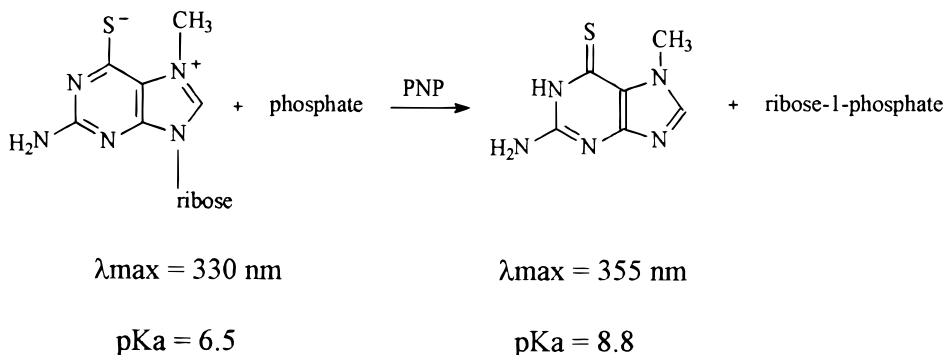
<sup>4</sup> To whom correspondence should be addressed. Fax: (734) 936-9463. E-mail: [cordeseh@umich.edu](mailto:cordeseh@umich.edu).



Discovery of inhibitors has been facilitated by knowledge of the three-dimensional structure of human PNP (7) and a series of careful and detailed, if not always mutually consistent, studies of kinetics and mechanism for this enzyme (1,8–17). The structure-based search for useful inhibitors of PNP has resulted in discovery of several compound classes (18–21), which was built on earlier studies (22–26). More recently, detailed structures of calf spleen PNP and its complexes with a number of substrates, substrate analogs, and inhibitors (27–29), as well as the structure of the *Escherichia coli* enzyme (30), have clarified several aspects of mechanism and catalysis for PNP and provided an expanded structural basis for inhibitor discovery.

The discovery of novel enzyme inhibitors having properties appropriate for clinical use is of general interest to this laboratory. Specifically, in collaboration with BioCryst Pharmaceuticals, Inc., we have initiated a program of research designed to discover structurally novel, and clinically useful, second-generation inhibitors of human PNP. The first phase of this work is the creation of a standard database of PNP inhibitor data and the development of predictive QSAR models based upon it.

At the outset of this work, we considered that 2-amino-6-mercapto-7-methylpurine ribonucleoside (MESG) might be a suitable substrate to employ in PNP inhibitor discovery. It has been established that this molecule is a substrate for PNP and the kinetics of its phosphorolysis (or hydrolysis) can be conveniently followed spectrophotometrically in the range 355–360 nm (31,32) (Scheme I).



SCHEME I

This substrate has been successfully employed to assay activities of enzymes in several classes (31,33,34). The assay derives from the change in  $\text{pK}_a$  for the conjugate acid of the purinethiol moiety of the ribonucleoside, 6.5, and for the conjugate acid of the free purinethiol, 8.8. Thus, at the value of pH employed in our studies, 7.4, about 89% of MESG is present in solution as the zwitterionic conjugate base,  $\lambda_{\max}$  330 nm, but about 96% of the purinethiol product is present as the neutral conjugate acid,  $\lambda_{\max}$  355 nm (31).

In the course of this work, we discovered a phosphate-independent hydrolysis of MESG catalyzed by calf spleen PNP and have established several features for the kinetics of this reaction. The results of this work are presented herein.

## RESULTS

*Nonenzymatic decomposition of MESG.* MESG is unstable in aqueous solution (31). In dilute aqueous acid, pH 2–3, we observed a half-life in the range of 20–30 days at room temperature. MESG is reasonably stable in dimethyl sulfoxide solution. The structure of the decomposition products is not known although the reaction presumably involves base-catalyzed attack on the cationic purine ring (35). The rate of nonenzymatic decomposition of MESG under the conditions of our measurements, pH 7.4 and 25°C, is sufficiently rapid to require correction of all kinetic measurements reported herein.

Since our kinetic measurements were made under zero-order conditions, we determined the zero-order rate of decomposition of MESG as a function of MESG concentration under our experimental conditions. Manually or employing the robotic workbench, zero-order rates for MESG decomposition were determined by following the increase in absorbance at 314 nm or the decrease in absorbance at 356 nm as a function of time over the concentration range 10–150 nM. Zero-order rates were found to be linearly dependent on MESG concentration:

$$\text{Rate}_{314\text{nm}}/\text{initial absorbance}_{330\text{nm}} = 2.4 \pm 0.2 \times 10^{-6} \text{ AU/s/AU},$$

$$\text{Rate}_{356\text{nm}}/\text{initial absorbance}_{330\text{nm}} = -4.0 \pm 1.0 \times 10^{-6} \text{ AU/s/AU}.$$

From time to time, control measurements were carried out to ensure that nonenzymatic decomposition rates were consistent with these values.

First-order rate constants for MESG decomposition were also determined at 25°C as a function of pH in the presence of 0.05 M tris-hydroxymethylaminomethane (Tris) buffer: pH 7.0,  $k_{\text{obs}} = 3 \times 10^{-5} \text{ s}^{-1}$ ; pH 7.4,  $k_{\text{obs}} = 4.3 \times 10^{-5} \text{ s}^{-1}$ ; pH 8.0,  $k_{\text{obs}} = 8 \times 10^{-5} \text{ s}^{-1}$ . At values of pH greater than 9, decomposition of MESG is rapid. These observations are in general accord with those of Webb (31) and Broom and Milne (36).

*Basic kinetic behavior of calf spleen PNP-catalyzed phosphorolysis of MESG.* At pH 7.4 (0.1 M *N*-(2-hydroxyethyl)piperazine-*N'*-(2-ethanesulfonic acid), sodium salt; Hepes), 25°C, and in the presence of 10 mM phosphate, zero-order rates for calf spleen PNP-catalyzed phosphorolysis of MESG were found to increase linearly with increasing PNP concentration over the concentration range 30–120 nM.

Zero-order rates for PNP-catalyzed phosphorolysis of MESG at pH 7.4 were determined as a function of MESG concentration (concentration range 35–280  $\mu\text{M}$ ) for two ranges of phosphate concentration: (a) 0.012–0.1 mM and (b) 0.3–4 mM. In each case, rates were determined at five concentrations of MESG at each of five concentrations of phosphate. These data were employed to calculate values for the apparent  $K_m$  for MESG and phosphate as a function of the concentration of the fixed varying substrate.

Values of apparent  $K_m$  for MESG showed modest dependence on phosphate concentration: The apparent  $K_m$  is near 100  $\mu\text{M}$  at 1 mM phosphate and near 400  $\mu\text{M}$  at very low phosphate concentrations. These values are consistent with one of 70  $\mu\text{M}$  determined by Webb (31) for a bacterial PNP at pH 7.6. Values of apparent  $K_m$  for

phosphate are slightly dependent on the concentration of MESG but are markedly dependent on the range of phosphate concentration employed for their determination. At low phosphate and low MESG concentrations, the apparent  $K_m$  for phosphate is in the range 50–60  $\mu\text{M}$ ; at high phosphate and low MESG concentrations, the apparent  $K_m$  is in the range 700–800  $\mu\text{M}$ . Webb (31) has reported an apparent  $K_m$  for phosphate of 25  $\mu\text{M}$  for a bacterial PNP at pH 7.6 and Porter has found a value of 140  $\mu\text{M}$  for the calf spleen enzyme (12), both consistent with our value determined at low phosphate concentrations. Ropp and Traut (11) found a higher value, 3.1 mM, for the  $K_m$  for phosphate for the calf spleen enzyme. Two apparent binding sites for phosphate on PNP have been previously described, based both on structural data for the human enzyme (7) and on kinetic data (11,12). However, a recent, detailed structure for the calf spleen enzyme reveals no evidence for a second phosphate binding site (27).

*Kinetics of calf spleen PNP-catalyzed hydrolysis of MESG in the absence of phosphate.* At concentrations of phosphate below about 1 mM, calf spleen PNP catalyzes the slow decomposition of MESG at a rate that is independent of phosphate concentration. This is not particularly surprising since PNP-catalyzed hydrolysis of inosine and guanosine in the absence of phosphate has been previously observed by Kline and Schramm (1,14). In addition, crystalline calf spleen PNP has been demonstrated to catalyze the hydrolysis of inosine (27). It is thus highly likely that the phosphate-independent reaction with MESG is also hydrolysis (a) by analogy with results of Kline and Schramm (1,14) and Mao *et al.* (27) and (b) through the identification of the purinethiol base derived from MESG as a reaction product based on an exact mass determination employing FAB mass spectrometry. However, we have not identified ribose as the other reaction product. As is detailed below, the phosphate-independent PNP-catalyzed decomposition of MESG terminates after a few catalytic turnovers, generating very limited amounts of products and making detection of ribose problematic. In what follows, we assume that the phosphate-independent decomposition reaction is, in fact, hydrolysis.

Zero-order rates for PNP-catalyzed hydrolysis of MESG were determined as a function of the concentration of substrate and enzyme. The ratio of zero-order rates and substrate concentration is collected for five concentrations of MESG varying from 1.07 to  $6.03 \times 10^{-5}$  M and five concentrations of PNP varying from 0.06 to 1.60  $\mu\text{M}$  (Table 1). Values of this ratio in each column of Table 1 are sensibly constant, indicating that the rates are linear in substrate concentration. This finding is consistent with the value of  $K_m$  for MESG at low phosphate of 400  $\mu\text{M}$  cited above. In the last row of Table 1, average values for these ratios have been divided by the concentration of PNP. Here too sensibly constant values are obtained, establishing that the rate of this reaction is linear in enzyme concentration.

In the course of these studies, it was observed that the reactions terminated well before all MESG substrate initially present was consumed. Data for the extent of hydrolysis as a function of PNP concentration are collected in Table 2. The extent of MESG hydrolysis increases with increasing enzyme concentration but less rapidly than linearly. In other words, the number of catalytic events per enzyme monomer decreases with increasing enzyme concentration (Table 2). Under the conditions of these experiments, the hydrolytic reaction terminates following 8–45 catalytic events

TABLE 1

The Ratio of Zero-Order Rates and Substrate Concentration for Calf Spleen PNP-Catalyzed Decomposition of MESG at pH 7.4 and 25°C<sup>a</sup>

[MESG] $\times 10^{-5}$ M	[PNP] <sup>b</sup> ( $\mu$ M)				
	0.06	0.18	0.30	0.78	1.60
1.07	3.81	7.42	13.6	36.2	77.1
2.15	2.72	7.86	14.8	31.3	65.1
2.68	3.95	7.95	12.5	30.4	60.4
3.75	3.28	8.21	13.1	29.3	61.9
6.03	4.20	9.02	13.7	30.5	59.8
Average	3.59	8.09	13.5	31.5	64.9
Average/[PNP] <sup>c</sup>	$6 \times 10^2$	$4.5 \times 10^2$	$4.5 \times 10^2$	$4.0 \times 10^2$	$4.1 \times 10^2$

<sup>a</sup> Ratios have units of s<sup>-1</sup> and have been multiplied by 10<sup>5</sup>.

<sup>b</sup> As the monomer.

<sup>c</sup> V/[MESG]/[PNP]; values have units of s<sup>-1</sup> M<sup>-1</sup>.

per enzyme monomer. As is detailed below, reaction termination is not the consequence of product inhibition.

In an effort to understand the central aspects of calf spleen PNP-catalyzed hydrolysis of MESG in the absence of phosphate, four complex experiments were designed and carried out.

The first experiment is characterized by an excess of enzyme over substrate. Specifically, four reactions were carried out employing 4  $\mu$ M MESG and 12  $\mu$ M PNP (as the monomer, 4  $\mu$ M as the trimer). One reaction originally contained 1 mM

TABLE 2

Extent of Hydrolysis of MESG Catalyzed by PNP as a Function of the Concentration of Enzyme at pH 7.4 and 25°C<sup>a</sup>

[PNP] <sup>b</sup> (μM)	MESG consumed (μM)	Percentage MESG initially present hydrolyzed	$\left(\frac{\text{Moles MESG hydrolyzed}}{\text{Moles PNP}}\right)_{\text{obs}}$	$\left(\frac{\text{Moles MESG hydrolyzed}}{\text{Moles PNP}}\right)_{\text{calc}}$
150 μM MESG				
0.06	2.70	1.8	45	45
0.18	5.70	3.8	32	29
0.30	6.86	4.6	23	23
0.78	9.12	6.1	12	14
1.60	13.5	9.0	8.4	9
60 μM MESG				
0.78	7.84	13.1	10	14
1.60	12.3	20.5	7.7	9

<sup>a</sup> As determined by the change in absorbance at 361 nm at reaction termination.

<sup>b</sup> As the monomer.

phosphate; the other three contained no added phosphate. Plots of absorbance at 356 nm as a function of time for these reactions, as well as subsequent manipulations of them, are depicted graphically in Fig. 1.

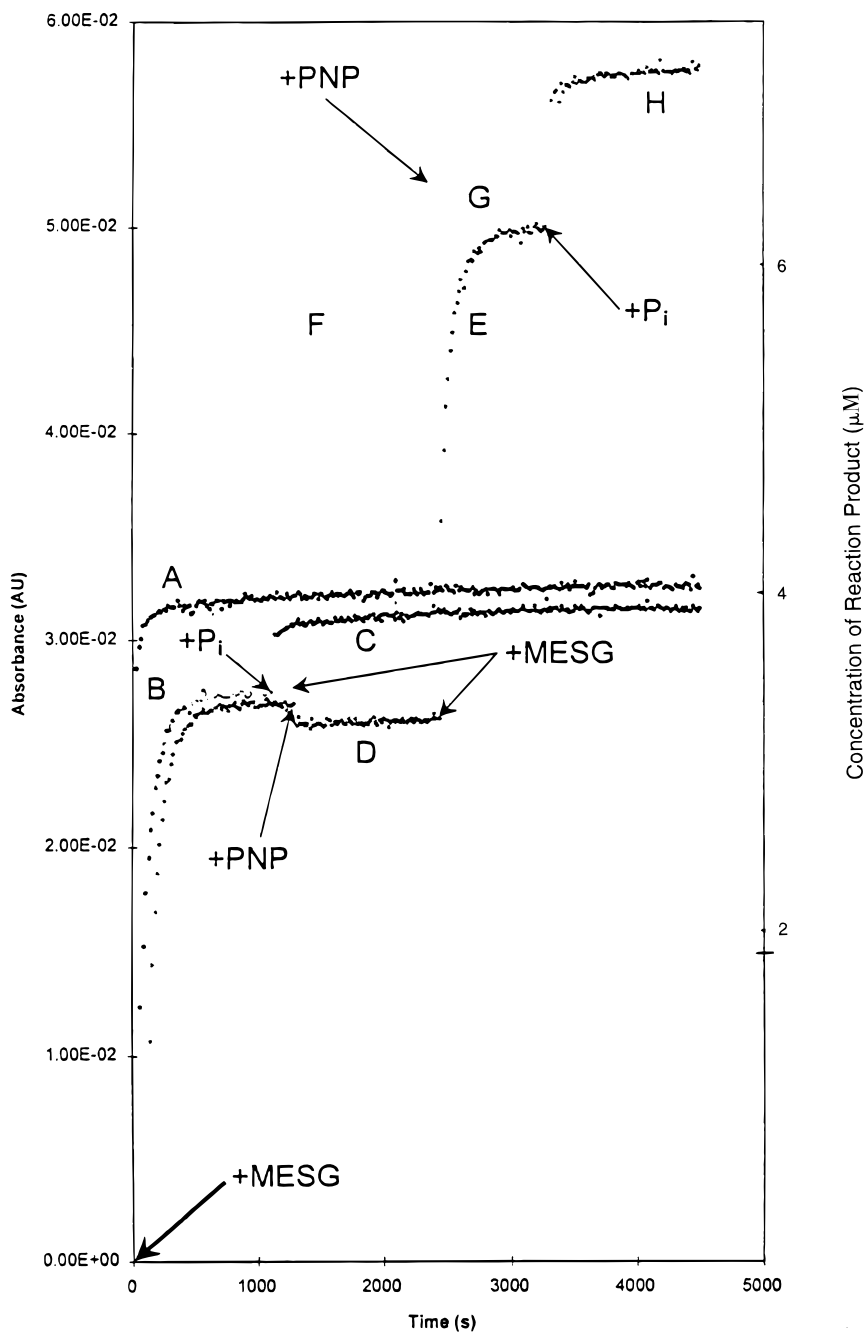
The reaction containing 1 mM phosphate (trace A, Fig. 1) proceeded rapidly to completion ( $k_{\text{obs}} > 0.1 \text{ s}^{-1}$ ) with a net change in absorbance of 0.032 AU, consistent with the absorbance calculated at this wavelength for a 4  $\mu\text{M}$  solution of the purinethiol product. Thus, all the MESG initially present was converted to products in the presence of 1 mM phosphate and excess enzyme, as expected. The three reactions without added phosphate (traces B; Fig. 1) proceeded more slowly (values of  $k_{\text{obs}}$  are  $0.0126 \pm 0.0006$ ,  $0.0117 \pm 0.0005$ , and  $0.0129 \pm 0.0006 \text{ s}^{-1}$  for the three runs) and with a slightly smaller net change in absorbance of 0.027 AU.

At the 1100-s time point, sufficient concentrated phosphate buffer was added to the first of these reactions to achieve a final phosphate concentration of 1 mM (trace C; Fig. 1); a small increase in absorbance to 0.031 AU which was too fast to follow by conventional means was observed. This value is not different from that observed for the reaction initially containing phosphate (0.032 AU) when correction is made for sample dilution and nonenzymatic decomposition of MESG. The phosphate-induced increase in absorbance may reflect: (a) displacement of product purinethiol from an enzyme-product complex by phosphate or (b) completion of an incomplete reaction driven by phosphate. The latter possibility seems unlikely in view of the excess of enzyme over substrate and the essential irreversibility of the hydrolytic reaction. It is definitively eliminated by results of the following two experiments.

First, to the second of the three non-phosphate-containing reactions was added a second aliquot of 12  $\mu\text{M}$  PNP (trace D, Fig. 1). Except for sample dilution, no change in absorbance was observed, consistent with the absence of unreacted MESG in the reaction mixture. Subsequent addition of 4  $\mu\text{M}$  MESG (trace E, Fig. 1) resulted in a reaction which occurred with an increase in absorbance of 0.024 AU. Second, to the last of the three non-phosphate reactions was added a second aliquot of 4  $\mu\text{M}$  MESG (trace F, Fig. 1). A subsequent reaction was observed with a first-order rate constant of  $0.0074 \pm 0.0006 \text{ s}^{-1}$  and a net absorbance increase of 0.025 AU, similar to that observed for the two reactions described above. Addition of 12  $\mu\text{M}$  PNP to this reaction resulted in no change in absorbance other than that consequent to sample dilution (trace G, Fig. 1), confirming again that no unreacted MESG remained in the reaction mixture. Finally, addition of sufficient concentrated phosphate to this reaction mixture to yield 1 mM phosphate resulted in an increase in absorbance of 0.07 AU (trace H, Fig. 1); roughly twice that observed for the reaction containing half as much

---

**FIG. 1.** Absorbance at 356 nm (left ordinate) and product concentrations (right ordinate) plotted as a function of time for four reaction mixtures initially containing 4  $\mu\text{M}$  MESG and 12  $\mu\text{M}$  PNP, pH 7.4, 25°C. The first reaction contained 1 mM phosphate (trace A). Three other reactions initially contained no phosphate (traces B). To the first of these reactions was added 1 mM phosphate at the indicated time point (trace C). To the second of these three were added successively 12  $\mu\text{M}$  PNP, 4  $\mu\text{M}$  MESG, and 1 mM phosphate at the indicated time points (traces D, E, and H). To the last of these three reactions were added successively 4  $\mu\text{M}$  MESG, 12  $\mu\text{M}$  PNP, and 1 mM phosphate at the indicated time points (traces F, G, and H).



MESG (see traces B and C, Fig. 1). Thus, this result is also consistent with and supports displacement by phosphate of product purinethiol from an enzyme-product complex.

The second experiment is closely related to the first and was designed to confirm and expand conclusions based on that experiment. In this case, only two reactions were run: the first contained 8  $\mu\text{M}$  MESG, 0.9  $\mu\text{M}$  PNP, and 1 mM phosphate. The second contained 8  $\mu\text{M}$  MESG, 12  $\mu\text{M}$  PNP, but no added phosphate. For both reactions, absorbance at 356 nm is plotted as a function of time in Fig. 2.

In the presence of phosphate, the absorbance at 356 nm increased rapidly,  $k_{\text{obs}} = 0.0320 \pm 0.0006 \text{ s}^{-1}$ , with a net absorbance increase of 0.057 AU (trace A, Fig. 2). This absorbance change is consistent with complete, or nearly complete, conversion of MESG to phosphorolysis products. A second addition of 8  $\mu\text{M}$  MESG to this reaction mixture resulted in a second reaction having a rate and absorbance change, 0.055 AU, very similar to that of the first (trace C, Fig. 2), as did a third addition of 8  $\mu\text{M}$  MESG (change in absorbance 0.055 AU) (trace E, Fig. 2) and a fourth such addition (change in absorbance 0.053 AU) (trace G, Fig. 2). These results establish that (a) the PNP remains fully active after repeated rounds of phosphorolysis of MESG in the presence of 1 mM phosphate and (b) product inhibition is not marked for this reaction (see below).

The behavior of the system is distinctly different in the absence of added phosphate. The initial reaction is slower,  $k_{\text{obs}} = 0.0102 \pm 0.0004 \text{ s}^{-1}$  (trace B, Fig. 2) (i.e., about 40 times less rapid than the corresponding reaction in the presence of 1 mM phosphate, correcting for the difference in PNP concentration) and occurs with a slightly smaller increase in absorbance (0.050 AU as opposed to 0.057 AU), in accordance with results of the first experiment (*vide supra*). Thus, all MESG initially present was converted to product in this reaction. A second addition of 8  $\mu\text{M}$  MESG resulted in a reaction (trace D, Fig. 2) characterized by a smaller absorbance increase, 0.026 AU. This increase reflects conversion of approximately 25% of the added MESG to products. A third such addition resulted in an absorbance increase of only 0.018 AU (trace F, Fig. 2), as did a fourth addition of MESG (trace H, Fig. 2). The last two increases are those expected on the basis of the addition of MESG alone, without conversion to product. Finally, sufficient phosphate buffer was added to the reaction mixture to yield a final phosphate concentration of 1 mM. A rapid increase in absorbance in 0.087 AU resulted (trace I, Fig. 2). This increase can be accounted for by the sum of two processes: the displacement of bound purinethiol from the enzyme by phosphate and the phosphorolysis of unreacted MESG remaining in solution. Quantitative agreement requires correction for nonenzymatic decomposition of MESG.

Thus, results of these two experiments are consistent with a model in which, in

---

**FIG. 2.** Absorbance at 356 nm (left ordinate) and product concentrations (right ordinate) plotted as a function of time for two reaction mixtures, pH 7.4, 25°C. The first reaction mixture initially contained 8  $\mu\text{M}$  MESG, 0.9  $\mu\text{M}$  PNP, and 1 mM phosphate (trace A). The second reaction mixture initially contained only 8  $\mu\text{M}$  MESG and 12  $\mu\text{M}$  PNP (trace B). To the first reaction mixture were added successively three aliquots of 8  $\mu\text{M}$  MESG (traces C, E, and G) at the indicated time points. To the second reaction mixture were added successively three aliquots of 8  $\mu\text{M}$  MESG and, finally, 1 mM phosphate (traces D, F, H, and I) at the indicated time points.



